Biomath Communications

www.biomathforum.org/biomath/index.php/conference

Effects of Temperature on Adaptive Processes in Simulated Chronic Inflammatory Demyelinating Polyneuropathy at 20°C–42°C [1]

D. I. Stephanova, M. Daskalova, A. Kossev
Institute of Biophysics and Biomedical Engineering
Bulgarian Academy of Sciences
dsteph@bio.bas.bg

Keywords: Temperature, Hypothermia, Hyperthermia, CIDP, Excitability parameters, Computational neuroscience.

Abstract

The effects of temperature (from 20°C to 42°C) on action and polarizing electrotonic potentials (nodal and internodal) and their current kinetics were previously studied by us in a simulated case of 70% chronic inflammatory demyelinating polyneuropathy (70% CIDP). To complete the cycle of our studies on adaptive processes in this case, the temperature effects on strength-duration time constant, rheobasic current and recovery cycle are investigated. The computations use our temperature dependent multi-layered model of the myelinated human motor nerve fibre and the temperature is increased from

[1] **Citation:** D. I. Stephanova, M. Daskalova, A. Kossev, Effects of Temperature on Adaptive Processes in Simulated Chronic Inflammatory Demyelinating Polyneuropathy at 20°C–42°C. Biomath Communications 2/2 (2015) http://dx.doi.org/10.11145/j.bmc.2015.12.181

20°C to 42°C. The results show that as the action and polarizing electrotonic potential parameters, these excitability parameters are more sensitive to the hyperthermia (≥ 40°C) and are most sensitive to the hypothermia (≤ 25°C), especially at 20°C, than at temperatures in the range of 28°C–37°C. With the increase of temperature from 20°C to 42°C, the strength-duration time constant decreases ~ 5.2 times, while it decreases ~ 3.5 times in the physiological range of 28°C–37°C. Conversely, the rheobasic current increases ~ 3.0 times from 20°C–42°C, while it increases ~ 1.2 times in the range of 28°C–37°C. As in the normal case, the behavior of axonal superexcitability in the CIDP case is complex in a 100 ms recovery cycle with the increase of temperature. The axonal superexcitability decreases with the increase of temperature during hypothermia and increases with the increase of temperature during hyperthermia, especially at 42°C. However, the superexcitability period in the CIDP case is followed by a late subexcitability period at 37°C only and the recovery cycles are with reduced superexcitability and without relative refractory periods in the range of 20°C–40°C. The present results are essential for the interpretation of mechanisms of excitability parameter changes obtained here and measured in CIDP patients with symptoms of cooling, warming and fever, which can result from alterations in body temperature. They suggest that the adaptive processes in CIDP patients are in higher risk during hypothermia than during hyperthermia.

1 Introduction

CIDP is an immune-mediated neuropathy [11] and is clinically defined as a symmetric polyneuropathy involving both proximal and distal muscles. It is characterized by symmetric proximal and distal muscle weakness and motor-dominant manifestation [1, 5, 8, 10]. This disorder is also characterized by systematic demyelination, which results in slowing or blocking of action potential conduction in motor and sensory nerves [8]. The temperature dependent strength-duration time

constants, rheobasic currents and recovery cycles of peripheral nerves have been measured in healthy subjects and patients with CIDP using a noninvasive technique of threshold tracing [2, 6]. They are being introduced into the clinic to provide information about nerve function and dysfunction. It is established that cooling from 35°C to 29°C increases the strength-duration time constant by 2.6% per °C in healthy subjects, while the relative refractory period increases by 7.8% per °C [7]. Also, following warming to 37°C, the strength-duration time constants in patients with CIDP are decreased, rheobasic currents are increased, and recovery cycles are with reduced axonal superexcitability, while following cooling from 37°C to 25°C, the changes in these excitability parameters are largely similar [12].

Recently, we have examined the effects of temperature in the range of 20°C–42°C on simulated nodal and internodal (paranodal and midinternodal) action potentials and their current kinetics of the myelinated human motor nerve fibre [4, 9, 24] and in a case of 70% CIDP [21]. The action potentials reflect conducting processes in the fibre, when it is activated by short duration (0.1 ms) threshold current stimuli. The results show that in this temperature range, all action potential parameters in the CIDP case, except for the conduction block at 45°C during hyperthermia ($\geq$ 40°C) worsen, specifically: (i) the conduction velocities and potential amplitudes are decreased; (ii) the afterpotentials and threshold stimulus currents required for the potential generation are increased; (iii) the current kinetics of action potentials is slowed, and (iv) the conduction block during hypothermia ($\leq$ 25°C) is at temperatures lower than 20°C.

We have also examined the temperature effects in the range of 20°C–42°C on simulated nodal and internodal (paranodal and midinternodal) polarizing electrotonic potentials and their current kinetics of the myelinated human motor nerve fibre [18] and of the case of 70% CIDP [20]. The electrotonic potentials reflect accommodative processes in the fibre, when it is activated by long-lasting (100 ms) subthreshold depolarizing and hyperpolarizing current stimuli. The results show that while the changes of electrotonic potentials and their current kinetics are largely similar for the physiological range of 28°C–

37°C, they are altered during hypothermia and hyperthermia in the normal and CIDP cases. The normal (at 37°C) resting membrane potential is further depolarized or hyperpolarized during hypothermia or hyperthermia, respectively, and the internodal current types defining these changes are the same for both cases. However, in the CIDP case, the lowest and highest critical temperatures for blocking of electrotonic potentials are 20°C and 39°C, while in the normal case the highest critical temperature for blocking of these potentials is 42°C. In the temperature range of 20°C–39°C, the relevant potentials in the CIDP case, except for the lesser value (at 39°C) in hyperpolarized resting membrane potential, are modified: (i) polarizing nodal and depolarizing internodal electrotonic potentials and their defining currents are increased in magnitude; (ii) inward rectifier (I_{IR}) and leakage (I_{Lk}) currents, defining the hyperpolarizing internodal electrotonic potential, are gradually increased with the rise of temperature from 20°C to 39°C, and (iii) the accommodation to long-lasting hyperpolarization is greater than to depolarization.

To complete the cycle of our studies on axonal excitability properties of the CIDP case axons, the temperature effects on strength-duration time constant, rheobasic current and recovery cycle are investigated in the case of adaptation. The results provide evidence that these excitability parameters, as the action and electrotonic potentials, are also more sensitive to the hyperthermia and are most sensitive to the hypothermia, especially at 20°C, than at temperatures in the range of 28°C–37°C. The aim of this study is also to discuss our results concerning the temperature effects on conducting, accommodative and adaptive processes in the normal and CIDP cases in the range of 20°C–42°C.

2 Methods

The simulations presented here apply our temperature dependent model of motor nerve axons [24]. It is derived from our previous multi-layered model [13], of the myelinated human motor nerve fibre, in which temperature coefficients (Q_{10}-values) were involved for the ionic currents

(nodal and internodal), as well as for the conductivities of axoplasm and periaxonal space. These conductivities are geometry-independent. The equilibrium potential values are also temperature corrected. The Q_{10}'s and related details were also thoroughly described and discussed in the Appendix of our previous paper [18]. This temperature dependent multi-layered model is applied here to the previously simulated case of 70% PSD (paranodal systematic demyelination). The analysis shows that mild (20%, 50%, 70%) and severe (90%) PSDs are specific indicators for CIDP [14, 16, 17, 22].

According to the definition for PSD given in these our studies, the demyelination is associated with a corresponding loss of the myelin end bulbs and the reduction (70% — in the present study) of the paranodal seal resistance (R_{pn}), defining 70% PSD (70% CIDP), is uniform along the fibre length. Our results are also consistent with the interpretation that immunological factors causing changes in the paranodal segments of the myelin sheath could be responsible for the clinical abnormalities obtained in CIDP. In the normal fibre, the R_{pn} is 140 MΩ. The strength-duration time constants, rheobasic currents and recovery cycles are investigated in the range of 20°C–42°C. The temperature is changed uniformly in each segment along the fibre length and a case of uniform temperature change is realized, in contrast to the case of local (focal) temperature change. This second case is realized in nerve excitability measurements where the skin temperature at the site of stimulation is measured. This indicates that skin temperature at the side of stimulation does not exactly reflect the temperature of the underlying nerve, even if it is adequate as a qualitative indicator of changed temperature. The remaining parameters of the temperature dependent model are the same as previously described for our multi-layered model [13, 23, 25] and some of them are as follows. The myelin sheath is presented as a series of 150 parallel interconnecting lamellae, which are simulated by altering 150 lipid and 150 aqueous layers. The human model axon comprises 30 nodes and 29 internodes. Each internode is divided into two paranodal and five internodal segments. The lengths of node, paranode and nodal center to nodal center are 1.5, 200 and 1400 μm. All calculations are carried out for fibres with

an axon diameter of 12.5 μm and an external fibre diameter of 17.3 μm.

The temperature dependent strength-duration curves, charge-duration curves, strength-duration time constants, rheobasic currents and recovery cycles are investigated in the case of adaptation. The action potentials in this case (i.e. in the case of intracellular current application delivered simultaneously to the center of each internodal segment) are simulated by adding a long-duration threshold or suprathreshold depolarizing current stimulus. These action potentials are superimposed in each nodal and internodal segment along the fibre length as a periodic kind of fibre polarization is realized. Such polarization of the fibre was first simulated by [15] in the human motor electrotonus model. For a given temperature, the threshold stimulus duration is increased in 0.025 ms steps from 0.025 ms to 1 ms, to obtain the strength-duration curves. These curves are not simple single-exponential functions, and the charge-duration curves are not linear. Due to this, a polynomial function of degree 2 (transfer parabola), which relates threshold charge (Q) to stimulus duration (t), provides an accurate fit of the data: $Q = a_2[t^2 + (a_1/a_2)t + a_0/a_2]$, where a_0, a_1, a_2 are the polynomial coefficients. The strength-duration time constant (chronaxie) is defined as the absolute value of the smallest square root of the function (i.e., only one of both direct intercepts of the regression curve on the duration axis has a biophysical sense and only this direct intercept will be shown on the charge-duration figures). The rheobasic current is defined as the final decreased threshold value, after which the action potential generation cannot be obtained with an increase in the stimulus duration.

For a given temperature, when two equal-duration stimuli are used in pairs, the action potential in response to the second (testing) stimulus in the refractory period may be greater or less than that to the first (conditioning) stimulus and depends on the conditioning-test intervals. To obtain the time course of recovery of the axonal excitability following a single stimulus (the recovery cycle), testing threshold current stimuli of 1 ms duration are delivered at conditioning-test intervals of $2 - 100$ ms after a suprathreshold conditioning current stimulus of

1 ms duration. The testing stimulus thresholds are calculated at 27 conditioning-test intervals and the intervals increase up to 100 ms in approximately geometric progression. Three stimulus combinations are tested: (i) first (conditioning) stimulus (duration 1 ms) is determined at threshold; (ii) suprathreshold conditioning stimulus (duration 1 ms) is calculated, which is by 5% increased of threshold; and (iii) first suprathreshold (conditioning) plus second (testing) threshold stimuli are used to be obtained the recovery cycle.

3 Results

3.1 Abnormalities in the strength-duration time constants, rheobasic currents and their mechanisms in the rages of 28°C–37°C and 20°C–42°C for the normal and CIDP cases

Comparison between the temperature dependent strength-duration curves (Fig.1 (a, b), first column) and charge-duration curves (Fig. 1(a, b), last column) of the human motor nerve fibres is presented for the normal (Fig. 1(a)) and CIDP (Fig. 1(b)) cases. Histograms are used to provide a better illustration of the strength-duration time constants (Fig. 1(c), on the left) and rheobasic currents (Fig. 1(c), on the right) for the normal (*hatched bars*) and CIDP (*unhatched bars*) cases. Also to provide a better illustration of the obtained changes, these examined parameters are presented in the physiological temperature range of 28°C–37°C (Fig. 1) and in the temperature range of 20°C–42°C (Fig. 2). The normal data are taken from [19], and are presented here for comparison only. In the almost superimposed strength-duration curves for the normal and CIDP cases (Fig. 1(a, b), first column), the threshold stimulus currents at 28°C are highest for the 0.025 ms stimulus and are lowest for the 1 ms stimulus. Conversely, in both cases, the threshold stimulus currents at 37°C are lowest for the 0.025 ms stimulus and are highest for the 1 ms stimulus (Fig. 1(a, b), last column). The strength-duration curves

are not simple single-exponential functions. Due to this their corresponding charge-duration curves are not straight lines (Fig. 1(a, b), last column). The strength-duration time constants become gradually shorter as the temperature is increased from 28°C to 37°C (Fig. 1(c), on the left) in the normal and CIDP cases. However, the strength-duration time constants are shorter in the CIDP case. There is an inverse relationship between the strength-duration time constants and rheobasic currents during this range and the rheobasic currents are longer in the CIDP case than in the normal one. The strength-duration time constants are $0.133, 0.114, 0.106, 0.095$ ms and rheobasic currents are $0.666, 0.717, 0.750$, and 0.800 nA at 28°C, 32°C, 34°C, and 37°C, respectively, in the CIDP case. The strength-duration time constants are $0.397, 0.351, 0.328, 0.291$ ms and rheobasic currents are $0.315, 0.340, 0.356, 0.388$ nA at 28°C, 32°C, 34°C, and 37°C, respectively, in the normal case.

The results show that the transition from 20°C to 42°C leads to amplification of the degree of above examined parameters in the normal and CIDP cases, as the direction of these changes is maintained (Fig. 2). The strength-duration time constants are longest (0.509 ms)/(0.196 ms) at 20°C and shortest (0.058 ms)/(0.038 ms) at 42°C in the normal and CIDP cases, respectively, while the rheobasic currents are lowest (0.283 nA)/(0.617 nA) at 20°C and highest (1.231 nA)/(1.861 nA) at 42°C in the same cases, respectively. The strength-duration time constants are 0.376 ms/0.123 ms and 0.159 ms/0.074 ms, while the rheobases are 0.327 nA/0.689 nA and 0.631 nA/1.193 nA at 30°C and 40°C in the normal and CIDP cases, respectively. Consequently, with the increase of temperature from 20°C to 42°C, the strength-duration time constant decreases ~ 5.2 times in the CIDP case, while it decreases ~ 3.5 times in the physiological range of 28°C–37°C. Conversely, the rheobasic current increases ~ 3.0 times from 20°C to 42°C, while it increases ~ 1.2 times in the range of 28°C–37°C. In the normal case, with the increase of temperature from 20°C to 42°C, the strength-duration time constant decreases ~ 8.6 times, while it decreases ~ 1.4 times in the physiological range of 28°C–37°C. Conversely, the rheobasic current increases ~ 4.3 times

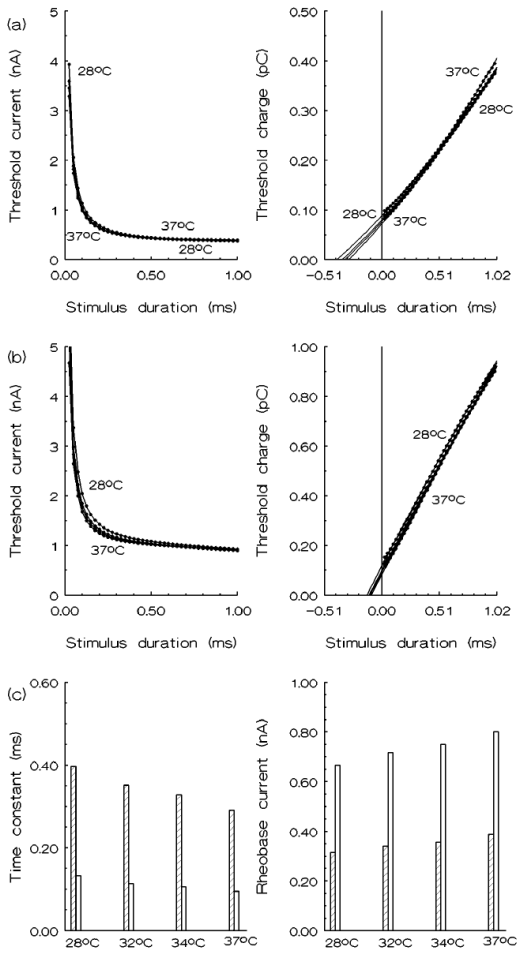

Figure 1: Comparison between the strength-duration curves ((a, b), first column) and charge-duration curves ((a, b), last column) for the normal (a) and CIDP (b) cases, as well as between the strength-duration time constants ((c), first column) and rheobasic currents ((c), last column) for the normal (*hatched bars*) and CIDP (*unhatched bars*) cases in the temperature range of 28°C–37°C. For both cases, the strength-duration curves and charge-duration curves almost superimpose and due to this the lowest and highest temperatures are only given in the first and second row panel figures.

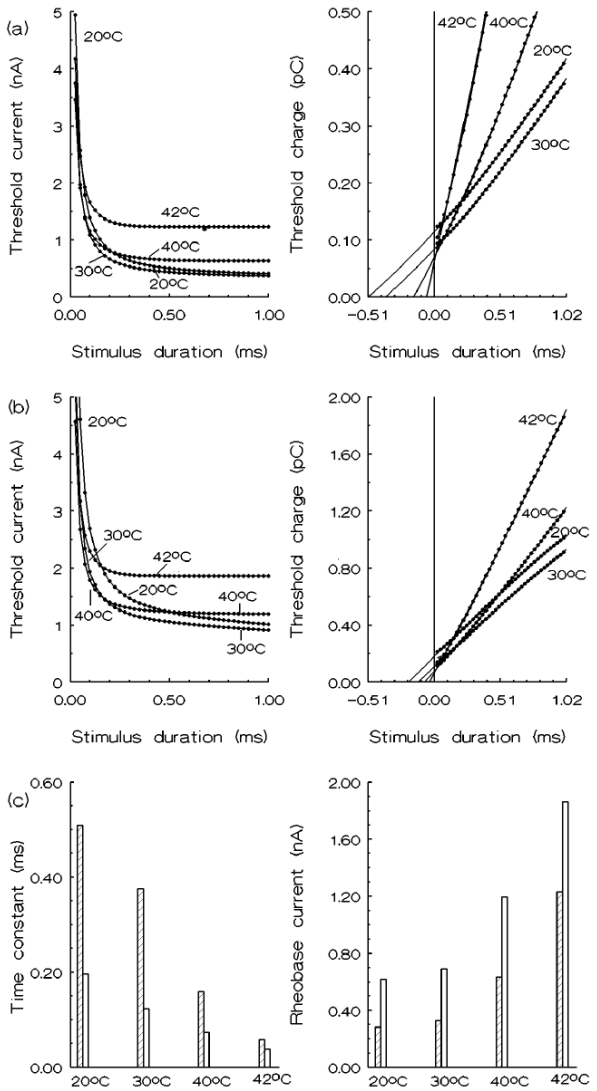

Figure 2: Comparison between the strength-duration curves ((a, b), first column) and charge-duration curves ((a, b), last column) for the normal (a) and CIDP (b) cases, as well as between the strength-duration time constants ((c), first column) and rheobasic currents ((c), last column) for the normal (*hatched bars*) and CIDP (*unhatched bars*) cases at temperatures given in the panel figures.

from 20°C to 42°C, while it increases ~ 1.2 times in the physiological range of 28°C–37°C.

3.2 Abnormalities in the recovery cycles and their mechanisms in the rage of 20°C–42°C

Absolute temperature dependent recovery cycles of the human motor nerve fibres in the normal (Fig. 3 (a)) and CIDP (Fig. 3 (b)) cases are plotted on logarithmic x-axes and linear y-axes. The horizontal lines in the panel figures indicate the control threshold current (i.e. suprathreshold current increased by 5% of threshold) of conditioning (first) stimuli. To clarify presentation, the recovery cycles and the control threshold currents of their corresponding conditioning stimuli are numbered from 1 to 6 and each consecutive number corresponds to a temperature from 20°C to 42°C. The recovery cycles are presented during hypothermia (20°C, first column in Fig. 3), the physiological range (30°C, first column in Fig. 3; 34°C and 37°C, second column in Fig. 3) and hyperthermia (40°C and 42°C, last column in Fig. 3). The data comparing two temperatures (20°C and 30°C, first column in Fig. 3; 34°C and 37°C second column in Fig. 3; and 40°C and 42°C, last column in Fig. 3) are given in each panel figure. The dotted curves and lines indicate the lower of the two temperatures. The normal data are taken from [19], where they were thoroughly described and discussed. They are presented here for comparison only. As for the normal case (Fig. 3 (a)), the data for the CIDP case (Fig. 3 (b)) clearly show that the effect of temperature on the conditioning control threshold current is complex. First, this current decreases with the increase of temperature from 20°C to 30°C, then slightly increases during the temperature range of 34°C–37°C and finally increases rapidly during hyperthermia, especially at 42°C. The effects of temperature on the recovery cycle are more conspicuous than on any of the other excitability calculated parameters. The behavior of the relative refractory period and axonal superexcitability in a 100 ms recovery cycle is also complex with the increase of temperature. In the normal case, the relative refractory period (i.e. the period after conditioning ac-

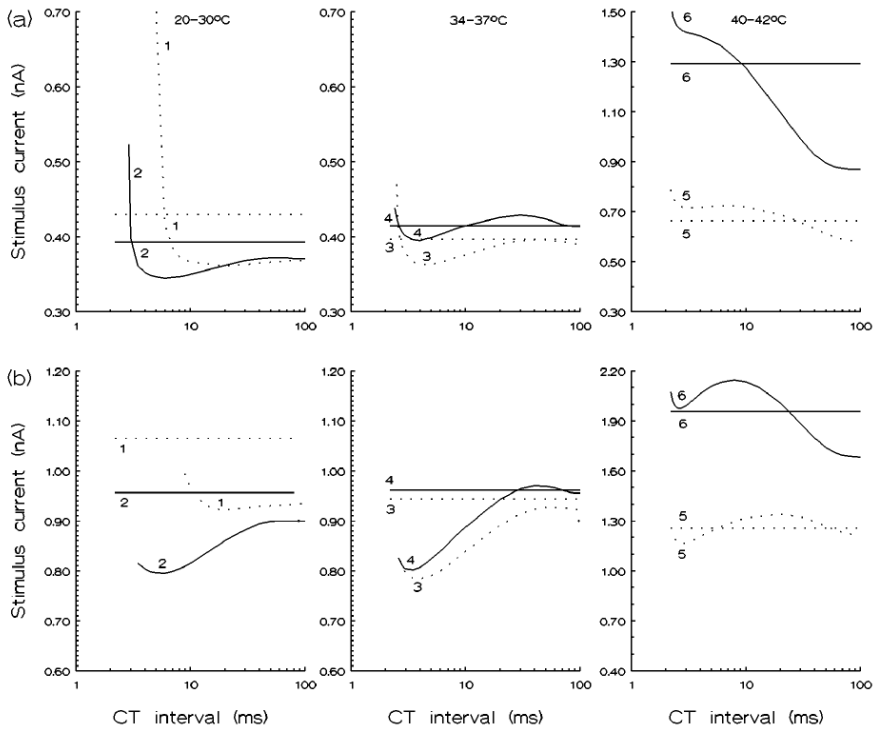

Figure 3: Comparison between the absolute recovery cycles of the myelinated human motor nerve fibre is presented in the normal (a) and CIDP (b) cases. The recovery cycles are numbered from 1 to 6 and each consecutive number corresponds to 20°C, 30°C, 34°C, 37°C, 40°C and 42°C, respectively. The recovery cycles are given in the temperature ranges of 20°C–30°C (first column), 34°C– 37°C (second column) and 40°C–42°C (last column). The dotted curves and lines indicate the lower of the two temperatures. The horizontal lines indicate the control threshold current (i.e. suprathreshold current increased by 5% of threshold) of the conditioning stimulus. Conditioning-test (CT) intervals are plotted on logarithmic x-axis scales.

tion potential during which threshold current of the testing stimulus is elevated), increases during hypothermia and decreases during the range of 30°C–37°C. It also increases during hyperthermia, especially at 40°C and after then decreases rapidly at 42°C. The refractoriness (i.e. the increase in threshold current during the relative refractory period) is highest at the lowest (20°C) temperature. It gradually decreases with the increase of temperature from 30°C to 37°C and then increases during hyperthermia. However, in the case of CIDP case, the recovery cycles are without relative refractory periods in the range of 20°C–40°C. The axonal superexcitability for both cases decreases with the increase of temperature during hypothermia. The axonal superexcitability increases rapidly with the increase of temperature during hyperthermia, especially at 42°C and a block of each applied third testing stimulus is obtained for the normal case. And a block of each applied second testing stimulus is obtained at temperatures higher than 42°C. However, in the CIDP case, a block of the applied testing stimuli is not obtained even at temperatures higher than 42°C. The axonal superexcitability period for the normal case is followed by a late subexcitability period when the temperatures are in the range of 32°C–37°C while, the superexcitability period for the CIDP case is followed by a late subexcitability period at 37°C only.

These recovery cycles are normalized and presented together in Fig. 4. For a given temperature, each recovery cycle is normalized to the control threshold current of its corresponding conditioning stimulus. The results show that for a given temperature the recovery cycles in the CIDP case are with reduced axonal superexcitabilities and are without relative refractory periods in the range of 20°C–40°C. The recovery cycles depend on the regenerative membrane depolarization or hyperpolarization caused by the conditioning afterpotential and could be explained by the delay-dependent testing potential (Figs. 5, 6 and 7). In these figures, the temporal distributions of temperature dependent testing action potentials in the case of adaptation as a function of conditioning-test (CT) intervals are compared between the normal (first and third columns in Figs. 5 and 6, and Fig. 7(a)) and CIDP (second and last columns in Figs. 5 and 6, and Fig. 7(b)) cases. Only

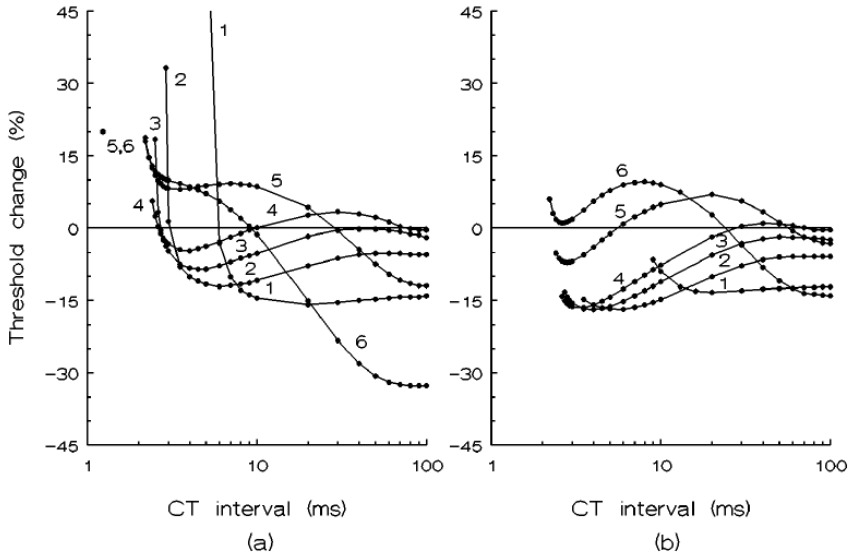

Figure 4: Comparison between the normalized recovery cycles of the myelinated human motor nerve fibre in the normal (a) and CIDP (b) cases. The recovery cycles are numbered from 1 to 6 and each consecutive number corresponds to 20°C, 30°C, 34°C, 37°C, 40°C and 42°C, respectively. For all cases, the y-axis is defined as $100(I_{\text{test}} - I_{\text{cond}})/I_{\text{cond}}$ (%), where I_{test} (nA) is the threshold current of the testing stimulus and I_{cond} (nA) is the control threshold current (i.e. suprathreshold current increased by 5% of threshold) of the conditioning stimulus. Conditioning-test (CT) intervals are plotted on logarithmic x-axis scales.

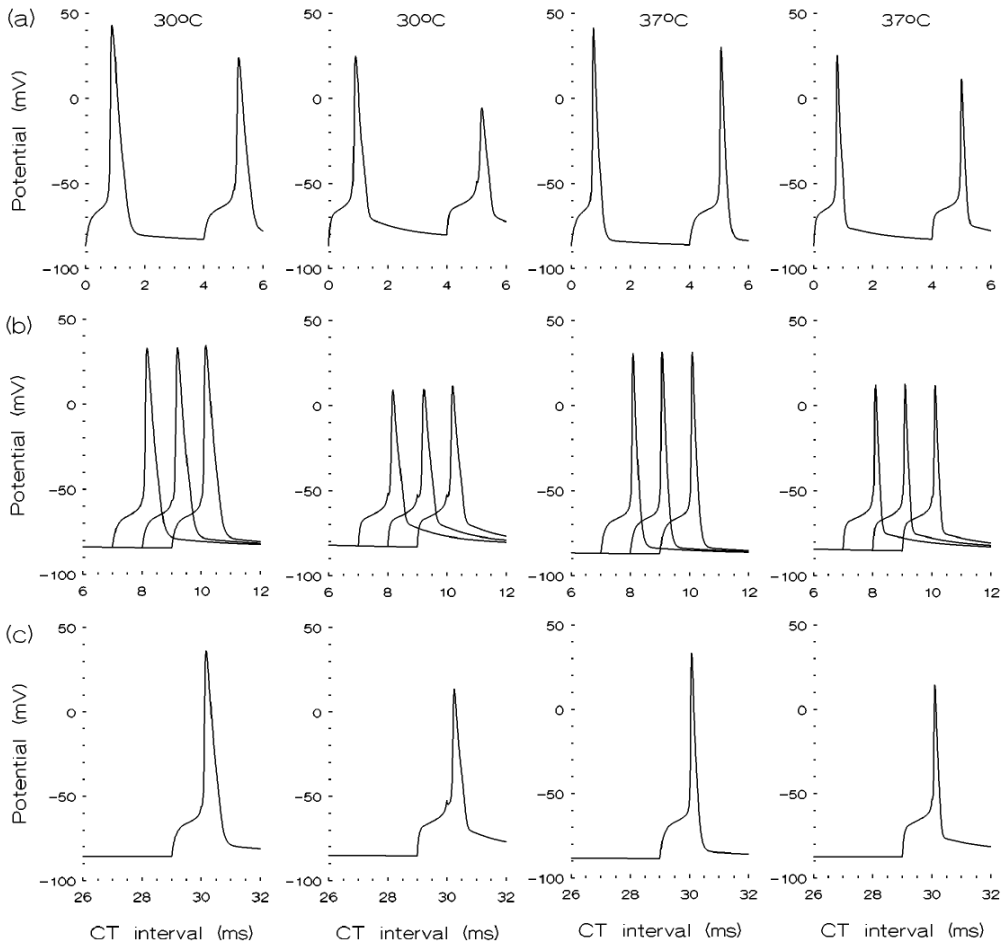

Figure 5: Comparison between the temporal distributions of action potentials in the case of adaptation, for the normal (first and third columns) and CIDP (second and last columns) cases, at temperatures given in the panel figure columns, when the testing stimulus is applied as a function of the conditioning-test (CT) intervals, corresponding to CT = 4 ms (a); CT = 7, 8 and 9 ms (b); and CT = 29 ms (c). The testing action potentials are compared with the conditioning action potentials only in (a) case (first row). The action potentials are presented at each node from the 7th to the 14th and at each internodal segment between them. However, these segments respond equally, as the periodic kind of fibre polarization is realized, and an overlap of the potentials in the nodal and internodal segments is obtained.

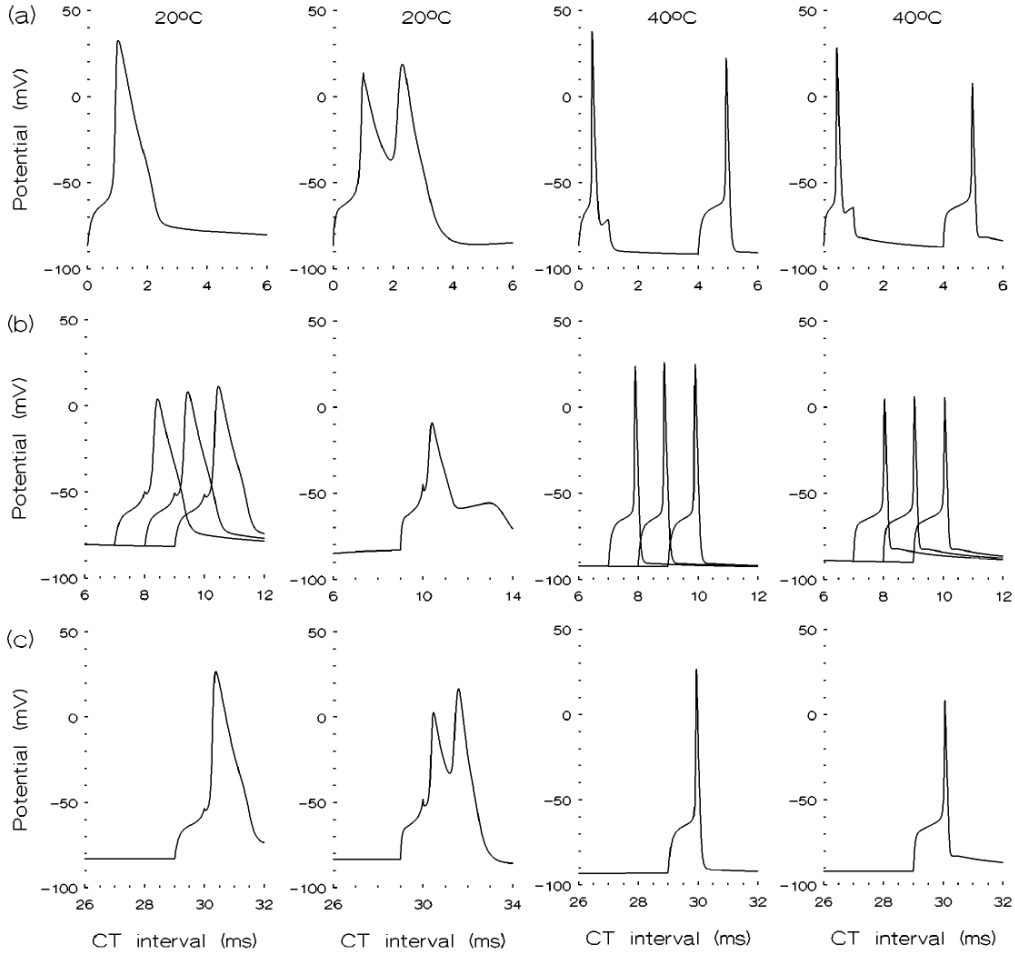

Figure 6: Comparison between the temporal distributions of action potentials in the case of adaptation, for the normal (first and third columns) and CIDP (second and last columns) cases, at temperatures given in the panel figure columns, when the testing stimulus is applied as a function of the conditioning-test (CT) intervals, corresponding to CT = 4 ms (a); CT = 7, 8 and 9 ms (b); and CT = 29 ms (c). The testing action potentials are compared with the conditioning action potentials only in (a) case (first row) except at 20°C for the normal and CIDP cases, where there were no testing potentials, as the axons are still in the absolute refractory period. Also, there were no testing action potentials corresponding to CT = 7 and 8 ms (b) at 20°C in the CIDP case, as the axon is still in the absolute refractory period; all else as in Fig.5 legend.

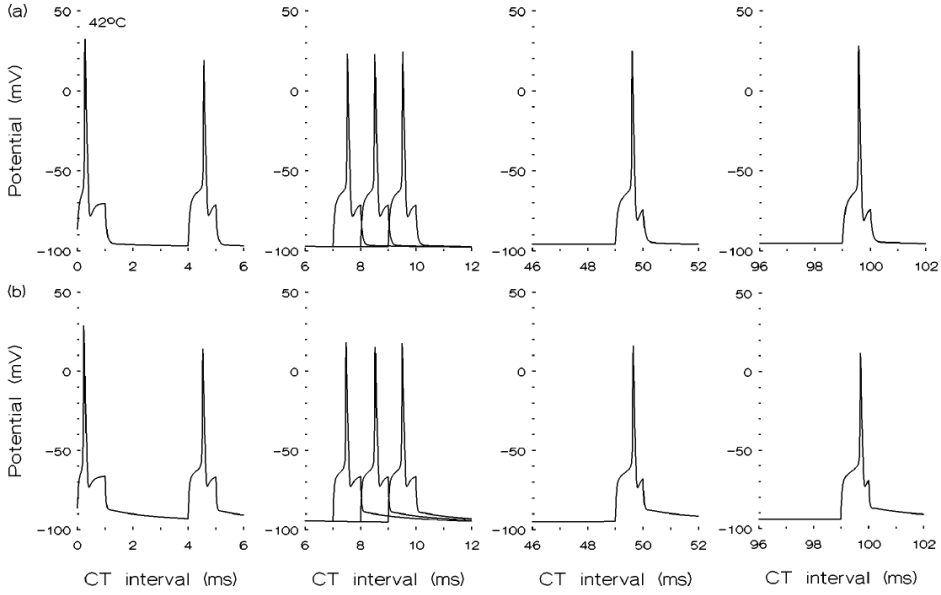

Figure 7: Comparison between the temporal distributions of action potentials in the case of adaptation for the normal (a) and CIDP (b) cases, at 42°C only, when the testing stimulus is applied as a function of the conditioning-test (CT) intervals, corresponding to CT = 4 ms (a); CT = 7, 8 and 9 ms (b); CT = 49 ms (c); and CT = 99 ms (d). For the normal and CIDP cases, the testing action potentials are compared with the conditioning action potentials only in the case when CT = 4 ms (first column); all else as in Fig.5 legend.

when the conditioning-test interval corresponds to 4 ms, the testing action potentials are compared with their conditioning potentials (Fig. 5(a), Fig. 6(a) and Fig. 7(first column)), except at 20°C for both cases in Fig. 6(a), where there were no testing potentials, as the axon is still in the absolute refractory period. The remaining testing action potentials are given at conditioning-test (CT) intervals corresponding to $7, 8, 9$ ms (Fig. 5(b), Fig. 6(b) and Fig. 7(second column)), 29 ms (Fig. 5(c) and Fig. 6(c)), 49 ms and 99 ms (Fig. 7 (third and last columns)). There were no testing action potentials corresponding to CT = 7 and 8 ms (Fig. 6(b)) at 20°C in the CIDP case, as the axon is still in the absolute refractory period. For the normal and CIDP cases, with the increase of temperature from 20°C to 42°C, the depolarizing conditioning afterpotentials decrease, reaching the normal (-86.7 mV) resting membrane potential and then they become hyperpolarized. The shape of conditioning and testing action potentials is abnormal at 42°C for both cases and it is abnormal at 20°C for the CIDP case only. Compared to the normal case, the depolarizing and hyperpolarizing afterpotentials are decreased smaller in the CIDP case.

4 Discussion

We have studied for the first time the effects of temperature on simulated strength-duration time constants, rheobasic currents and recovery cycles in the case of 70% CIDP, when the temperature is changed in a wide range of 20°C–40°C. The obtained data are compared to those for the normal case. The principle finding for both cases is that these excitability parameters are not very sensitive to temperature over the range encountered clinically. This result is in good agreement with nerve excitability studies on control groups [3, 6, 7] and patients with CIDP [12] focused on either cooling (to 28°C) or small deviations around normal (32°C or 35°C) skin temperature measured close to the site of stimulation during the test. The axonal excitability parameter changes obtained in the CIDP case are consistent with the effect of uniformly reduced paranodal seal resistance and uniformly

changed temperature along the fibre length.

A new finding in the present and our previous studies for the CIDP case [20, 21] is that the axonal excitability parameters (i.e. action, polarizing electrotonic potentials, strength-duration time constant, rheobasic current and recovery cycle) are more sensitive during hyperthermia and are most sensitive during hypothermia, especially at 20°C. The results confirm also that 20°C is the lowest critical temperature for patients with CIDP, as: (i) the abnormal action potentials (in the case of propagation and adaptation) have a bifid form and the conduction block during hypothermia is at temperatures lower than 20°C and (ii) the polarizing electrotonic potentials are in higher risk for blocking during hypothermia than during hyperthermia, The lowest critical temperature for healthy subjects is lower than 20°C. Conversely, for the normal case, our previous studies [4, 9, 18, 19] show that the same axonal excitability parameters are more sensitive during hypothermia and are most sensitive during hyperthermia, especially at 42°C. The results confirm also that 42°C is the highest critical temperature for healthy subjects, as: (i) the abnormal action afterpotentials (in the case of propagation and adaptation) are more hyperpolarized than those in the CIDP case and (ii) the polarizing electrotonic potentials are in higher risk for blocking during hyperthermia than during hypothermia. In the normal case, the axonal superexcitability in the 100 ms recovery cycle leads to blockage of each applied third testing stimulus at 42°C and to blockage of each applied second testing stimulus at temperatures higher than 42°C, while a block of applied testing stimulus is not obtained at 42°C and higher temperatures in the case of CIDP. The strength-duration time constant is shortest and the rheobasic current is highest at 42°C in the CIDP case. The mechanisms of abnormalities of above discussed excitability parameters were thoroughly described by their defining current kinetics in our previous studies [4, 9, 18, 19, 20, 21].

In summary, our results show that the temperature effects on the axonal excitability properties in the CIDP case are complex in the range of 20°C–42°C. Our studies provide a significant advance in knowledge as the results are essential for the interpretation of mecha-

nisms of temperature dependent nerve excitability properties in CIDP patients with symptoms of cooling, warming and fever, which can result from alterations in body temperature.

References

[1] R. J. Barohn, J.T. Kissel, J. R. Warmolts and J. R. Mendell, *Chronic inflammatory demyelinating polyradiculoneuropathy. Clinical characteristics, course, and recommendations for diagnostic criteria*, Arch Neurol. **46**(8):878-884, 1989.

[2] H. Bostock, K. Cikurel and D. Burke, *Threshold tracking techniques in the study of human peripheral nerve* (Review) Muscle Nerve **21**:137-158, 1998.

[3] D. Burke, I. Mogyoros, R. Vagg and M. C. Kiernan, *Temperature dependence of excitability indices of human cutaneous afferents*, Muscle Nerve **23**:51-60, 1999.

[4] M. Daskalova, S. Krustev and D. Stephanova, *Temperature effects on simulated human nodal action potentials and their defining current kinetics*, Scripta Scientifica Medica, **45**(3):42-47, 2013.

[5] P.J. Dyck, A. C. Lais, M. Ohta, J. A. Bastron, H. Okazaki and R. V. Groover, *Chronic inflammatory polyradiculoneuropathy*, Mayo Clin Proc. **50**(11):621-637, 1975.

[6] M. C. Kiernan, D. Burke, K.V. Andersen and H. Bostock, *Multiple measures of axonal excitability: a new approach in clinical testing*, Muscle Nerve, **23**:399-409, 2000.

[7] M. C. Kiernan, K. Cikurel and H. Bostock, *Effects of temperature on the excitability properties of human motor axons*, Brain **124**:816-825, 2001.

[8] H. Köller, B. C. Kieseier, S. Jander and H. P. Hartung, *Chronic inflammatory demyelinating polyneuropathy*, N Engl J Med. **352**(13):1343-1356, 2005.

[9] S. Krustev, M. Daskalova and D. Stephanova, *Temperature effects on simulated human internodal action potentials and their defining current kinetics*, Scripta Scientifica Medica **45**(4):36-40, 2013.

[10] S. Kuwabara and S. Misawa, *Chronic inflammatory demyelinating polyneuropathy: Clinical subtypes and their correlation with electrophysiology*, Clinical and Experimental Neuroimmunology **2**:41-48, 2011.

[11] K. Rezania, B. Gundogdu and B. Soliven, *Pathogenesis of chronic inflammatory demyelinating polyradiculoneuropathy*, Front Biosci. **9**:939-945, 2004.

[12] D. C. G. Straver, L. van Schelven, L. van den Berg and H. Franssen, *Interpretation of excitability studies in multifocal motor neuropathy and chronic inflammatory demyelinating polyneuropathy*, In: D.C.G. Straver, Mechanisms of conduction block in immune-mediated polyneuropathies. PhD Thesis, Utrecht University, The Netherlands, pp. 75-90, 2013.

[13] D. I. Stephanova, *Myelin as longitudinal conductor: a multilayered model of the myelinated human motor nerve fibre*, Biol Cybern. **84**:301-308, 2001.

[14] D. I. Stephanova and A.S. Alexandrov, *Simulating mild systematic and focal demyelinating neuropathies: membrane property abnormalities*, J Integr Neurosci. **5**(4):595-623, 2006.

[15] D. I. Stephanova and H. Bostock, *A distributed-parameter model of the myelinated human motor nerve fibre: temporal and spatial distributions of electrotonic potential and ionic currents*, Biol Cybern. **74**:543-547, 1996.

[16] D. I. Stephanova and M. Daskalova, *Differences in potentials and excitability properties in simulated cases of demyelinating neuropathies. Part II. Paranodal demyelination*, Clin Neurophysiol. **116**(5):1159-1166, 2005.

[17] D. I. Stephanova and M. Daskalova, *Membrane property abnormalities in simulated cases of mild systematic and severe focal demyelinating neuropathies*, Eur Biophys J. **37**(2):183-195, 2008.

[18] D. I. Stephanova and M. Daskalova, *Effects of temperature on simulated electrotonic potentials and their current kinetics of human motor axons at* $20^\circ C$–$42^\circ C$, J Integr Neurosci. **13**(3):447-464, 2014.

[19] D. I. Stephanova and M. Daskalova, *Theoretical predication of the effects of temperature on simulated adaptive processes in human motor nerve axons at* $20^\circ C$–$42^\circ C$, J Integr Neurosci. **13**(3):529-543, 2014.

[20] D. I. Stephanova and M. Daskalova, *Electrotonic potentials in simulated chronic inflammatory demyelinating polyneuropathy at* $20^\circ C$–$42^\circ C$, J Integr Neurosci. **14**(2):235-252, 2015.

[21] D. I. Stephanova and M. Daskalova. M. Mladenov, *Conducting processes in simulated chronic inflammatory demyelinating polyneuropathy at* $20^\circ C$–$42^\circ C$, J Integr Neurosci. **14**(1):19-30, 2015.

[22] D. I. Stephanova and B. Dimitrov, *Simulated demyelinating neuropathies and neuronopathies*, in: D.I. Stephanova & B. Dimitrov, eds., Computational Neuroscience: Simulated Demyelinating Neuropathies and Neuronopathies, Boca Raton (USA), CRC Press, Taylor and Francis Group, pp. 33-93, 2013.

[23] D. I. Stephanova and B. Dimitrov, *Models and methods for investigation of the human motor nerve fibre*, in: D.I. Stephanova & B. Dimitrov, eds., Computational Neuroscience: Simulated Demyelinating Neuropathies and Neuronopathies, Boca Raton (USA): CRC Press, Taylor and Francis Group, pp. 18-32, 2013.

[24] D. I. Stephanova, M. Daskalova and S. Krustev, *Modified multilayered model of temperature dependent motor nerve axons*, Scripta Scientifica Medica **45**(3):36-41, 2013.

[25] D. I. Stephanova, S. M. Krustev and N. Negrev, *Mechanisms defining the action potential abnormalities in simulated amyotrophic lateral sclerosis*, J Integr Neurosci. **11**(2):137-154, 2012.